

RESEARCH ARTICLE

Deregulation of LRSAM1 expression impairs the levels of TSG101, UBE2N, VPS28, MDM2 and EGFR

Anna Minaidou^{1,2}, Paschalis Nicolaou^{1,2}, Kyproula Christodoulou^{1,2*}

1 Neurogenetics Department, The Cyprus Institute of Neurology and Genetics, Nicosia, Cyprus, **2** Cyprus School of Molecular Medicine, Nicosia, Cyprus

* roula@cing.ac.cy



OPEN ACCESS

Citation: Minaidou A, Nicolaou P, Christodoulou K (2019) Deregulation of LRSAM1 expression impairs the levels of TSG101, UBE2N, VPS28, MDM2 and EGFR. *PLoS ONE* 14(2): e0211814. <https://doi.org/10.1371/journal.pone.0211814>

Editor: Matthew Seaman, Cambridge University, UNITED KINGDOM

Received: October 18, 2018

Accepted: January 22, 2019

Published: February 6, 2019

Copyright: © 2019 Minaidou et al. This is an open access article distributed under the terms of the [Creative Commons Attribution License](https://creativecommons.org/licenses/by/4.0/), which permits unrestricted use, distribution, and reproduction in any medium, provided the original author and source are credited.

Data Availability Statement: All relevant data are within the manuscript and its Supporting Information files.

Funding: This work was supported by a grant of the Cyprus TELETHON (Grant number: 73115). The funders had no role in study design, data collection and analysis, decision to publish, or preparation of the manuscript.

Competing interests: The authors have declared that no competing interests exist.

Abstract

CMT is the most common hereditary neuromuscular disorder of the peripheral nervous system with a prevalence of 1/2500 individuals and it is caused by mutations in more than 80 genes. LRSAM1, a RING finger ubiquitin ligase also known as TSG101-associated ligase (TAL), has been associated with Charcot-Marie-Tooth disease type 2P (CMT2P) and to date eight causative mutations have been identified. Little is currently known on the pathogenic mechanisms that lead to the disease. We investigated the effect of LRSAM1 deregulation on possible LRSAM1 interacting molecules in cell based models. Possible LRSAM1 interacting molecules were identified using protein-protein interaction databases and literature data. Expression analysis of these molecules was performed in both CMT2P patient and control lymphoblastoid cell lines as well as in *LRSAM1* and *TSG101* downregulated SH-SY5Y cells. *TSG101*, *UBE2N*, *VPS28*, *EGFR* and *MDM2* levels were significantly decreased in the CMT2P patient lymphoblastoid cell line as well as in *LRSAM1* downregulated cells. *TSG101* downregulation had a significant effect only on the expression of *VPS28* and *MDM2* and it did not affect the levels of LRSAM1. This study confirms that LRSAM1 is a regulator of *TSG101* expression. Furthermore, deregulation of LRSAM1 significantly affects the levels of *UBE2N*, *VPS28*, *EGFR* and *MDM2*.

Introduction

Charcot-Marie-Tooth (CMT) disease is the most common inherited neuropathy, characterized by peripheral nervous system degeneration, with a relatively high frequency (1:2,500 individuals) [1,2]. CMT disease is classified into demyelinating, axonal and intermediate types based on electrophysiological findings [3]. It is further sub-divided into an increasing number of genetic subtypes with more than 80 CMT genes currently known.

Leucine Rich Repeat And Sterile Alpha Motif Containing 1 (LRSAM1) has been associated with Charcot-Marie-Tooth disease type 2P (CMT2P). LRSAM1, is a RING finger ubiquitin ligase, which participates in a range of functions, including cell adhesion, signaling pathways and cargo sorting through receptor endocytosis [4,5]. It is a multidomain protein with an N-terminal leucine-rich repeat (LRR) domain, followed by an Ezrin-Radixin-Moesin (ERM)

domain, a coiled-coil (CC) region, a SAM domain, a PSAP/PTAP tetrapeptide motif and a RING finger domain [6]. LRSAM1, also known as TAL (TSG101-associated ligase), regulates the levels of *TSG101* (Tumor Susceptibility gene 101) by polyubiquitination [7]. *TSG101* is a tumor suppressor gene component of the ESCRT machinery (Endosomal Sorting Complex Required for Transport), with a significant role in cell cycle regulation and differentiation [5,8]. LRSAM1 binds to TSG101, through a bivalent binding of the PTAP motif and the CC domain of LRSAM1 [5,9]. After binding, LRSAM1 attaches several monomeric ubiquitins to the C-Terminal of TSG101, thus regulating its function. LRSAM1 mutations impair the LRSAM1-TSG101 interaction [10].

We identified a dominant *LRSAM1* mutation (c.2047-1G>A, p.Ala683ProfsX3) located in the RING finger domain of LRSAM1 [11]. Recently, we reported that downregulation of *LRSAM1* affects the proliferation and morphology of neuroblastoma SH-SY5Y cells, and, over-expression of wild-type *LRSAM1* rescues, while the c.2047-1G>A mutant fails to rescue the phenotype of the cells [12]. To date, eight LRSAM1 mutations have been associated with CMT neuropathy, seven of them associated with dominant and one with recessive inheritance [13].

In order to study the role of *LRSAM1* and the effect of the c.2047-1G>A mutant E3 ligase domain, we identified molecules that possibly interact with LRSAM1. Expression levels of selected molecules were evaluated in the *LRSAM1* c.2047-1G>A CMT2P patient lymphoblastoid cell line and also in *LRSAM1* knocked down SH-SY5Y cells. Since, *TSG101* is the only currently well characterized interactor of LRSAM1 [5], we also knocked down *TSG101* in SH-SY5Y cells and evaluated the levels of selected molecules in these cells as well.

Materials and methods

In this study, we selected possible LRSAM1 interacting molecules and investigated their expression levels in CMT2P patient derived lymphoblastoid cell lines as well as in *LRSAM1* and *TSG101* downregulated neuroblastoma SH-SY5Y cells. This study was approved by the National Bioethics Committee of Cyprus (EEBK/ΕΠ/2013/28). Written informed consent was obtained from the participating CMT2P patient.

Cell culture

Lymphoblastoid cell cultures. Lymphoblastoid cell lines were established from a CMT2P patient and three normal control individuals after informed consent, using peripheral blood. The normal control individuals were sex and age matched with the CMT2P patient. Lymphocytes were collected from peripheral blood using Ficoll-Paque Plus (Sigma-Aldrich, USA). Selected lymphocytes were infected with the Epstein-Barr virus (EBV) and were cultured in DMEM medium supplemented with 2% FBS.

Human SH-SY5Y neuroblastoma cells culture. Human SH-SY5Y neuroblastoma cells (ECACC, Sigma-Aldrich, U.S.A.), were cultivated in Dulbecco's Modified Eagle Medium DMEM (Invitrogen, U.S.A.) growth medium without L-glutamine. The DMEM medium was supplemented with 10% FBS (Invitrogen, U.S.A.), 2% GlutaMAX (Gibco, U.S.A.) and 1% Penicillin-Streptomycin 100X Solution (Invitrogen, U.S.A.). Medium was changed every 2 or 3 days and 0.25% Trypsin-EDTA (Life Technologies, U.S.A.) was used for routine splitting of the cell culture. Both cell lines were incubated in a humidified atmosphere under 5% CO₂ at 37°C.

Whole human LRSAM1 constructs

The pIRES2-EGFP-*LRSAM1* wild-type and mutant constructs were purchased from Eurofins (Germany) as previously described [12]. The mutant *LRSAM1* cDNA construct included a G base deletion at the first base of exon 25, creating the frame shift at the RNA level [11].

Downregulation of LRSAM1 or TSG101 in neuroblastoma SH-SY5Y cells

Transfections were performed using Lipofectamine 3000 (C3019H, Life Technologies, U.S.A.) The siRNAs against *LRSAM1* or *TSG101* (Life Technologies, USA) were double-transfected into SH-SY5Y cells as previously described [12] and according to the manufacturer's instructions. The appropriate amount of siRNA and Lipofectamine 3000 were dissolved separately in the Opti-MEM reduced serum medium (Life Technologies, U.S.A.) without FBS and antibiotics. Negative control siRNA (Life Technologies, USA), lipofectamine only and untransfected cells were used as controls of the experiments. Twenty-four hours after each transfection, medium was replaced with fresh DMEM medium. Cells were harvested 96 hours after the first transfection for protein and RNA extraction.

Protein-protein interaction database

In silico analysis was carried out using the STRING9.05&10.0 (<http://string-db.org/>) and IntAct (<http://www.ebi.ac.uk/intact/>) databases in order to identify possible molecules that possibly interact with LRSAM1. Extracted LRSAM1 possibly interacting molecules were selected for RNA expression analysis after literature evaluation.

RNA isolation and cDNA synthesis from experimental SH-SY5Y cells and lymphoblastoid cell lines

Cells were collected in PBS and total RNA was isolated using the Qiagen RNeasy kit (Qiagen, U.S.A.). 1% β -Mercaptoethanol (Sigma-Aldrich, U.S.A.) was added in lysis buffer before use. Whole cDNA was synthesized using the ProtoScript First Strand cDNA Synthesis Kit (New England Biolabs, U.K.) using the oligo-dT primer d(T)23VN according to the manufacturer instructions.

RNA expression levels

Expression levels of the selected molecules were evaluated by cDNA PCR amplifications. At least two sets of primers specific for each molecule and also for the *GAPDH* housekeeping gene were used. For each set of primers a standard curve was plotted in order to define the optimum number of PCR reaction cycles that fall within the exponential phase of the amplification reaction (S1 Fig). RNA levels from the patient and control derived lymphoblastoid samples as well as from the LRSAM1 and TSG101 knocked down cells were normalized using the *GAPDH* housekeeping RNA levels. Gel bands were measured using the ImageJ analysis software.

Protein extraction from experimental SH-SY5Y cells and lymphoblastoid cell lines

Proteins were extracted using a protein lysis buffer, that contained 1M NaCl, 10mM Tris-Cl (pH = 7.5), 10% glycerol (G5516, Sigma-Aldrich, U.S.A.), 1% Tween20 (Affymetrix, U.S.A.), 10Mm β -Mercaptoethanol (Sigma-Aldrich, U.S.A) and 1x EDTA-free Protease Inhibitor Cocktail (Promega, U.S.A.). Cell lysates were centrifuged at 4°C and supernatants were collected. Lysates were sonicated and denatured at 95°C. Then proteins were diluted in 1x Sodium Dodecyl Sulfate 20% (ThermoFisher Scientific, U.K.). The Coomassie Plus (Bradford) protein assay (23236, ThermoFisher Scientific, U.K.) was used to determine the protein concentration.

Western blot analysis

Proteins from each sample were loaded and separated onto SDS-PAGE 12% polyacrylamide gels and were transferred to Hybond-P hydrophobic polyvinylidene difluoride (PVDF)

membranes (Millipore, Germany). Membranes were blocked for 1 hour at room temperature and were incubated overnight at 4°C with the respective specific primary antibody for each protein [mouse anti-LRSAM1/Abcam ab73113 (1:400), rabbit anti-LRSAM1/Novus Biological H00090678-D01 (1:750), mouse anti-TSG101/Novus Biological NB200-11 (1:500) and mouse anti- β -ACTIN/Sigma-Aldrich A2228 (1:4000)]. Then, incubation with the appropriate secondary antibodies was performed for 2 hours and followed by incubation with the visualization LumiSensor Chemiluminescent HRP Substrate Kit (Genscript, U.S.A.) at room temperature. Membranes were visualized using the UVP imaging system (BioRad, U.S.A.). Quantification of Western blots was performed using the ImageJ program (<https://imagej.nih.gov>). The protein quantity ratio was estimated relative to β -Actin.

Statistical analysis

Quantitative data (ratio %) from three independent experiments were analyzed using the two-tailed Student's paired t-test. Thresholds of P-value < 0.05 were considered statistically significant. All the data are expressed as the mean% \pm standard deviation (SD) from three independent experiments. The mean of quantitative data of the control samples was set to 100%.

Results

Deregulation of LRSAM1 affects TSG101 expression

Since TSG101 is an already known interactor of LRSAM1, we evaluated TSG101 levels in the CMT2P patient lymphoblastoid cell line. Western blot analysis of the CMT2P patient and two control individuals lymphoblastoid cell lines confirmed the presence of the wild-type and the mutant truncated LRSAM1 proteins in the patient sample, as previously reported (4), and revealed a more than 50% reduction of TSG101 levels in the patient lymphoblastoid cell line as compared with the controls (Fig 1).

With another approach, double transfection of *LRSAM1* siRNA in neuroblastoma SH-SY5Y cells caused a >70% decrease of LRSAM1 levels which also resulted to an approximately 50% reduction of TSG101 levels. Double transfection of *TSG101* siRNA caused a 70% decrease on TSG101 levels, while it did not affect the LRSAM1 levels (Fig 2).

Protein-protein interaction network extraction of LRSAM1 possibly interacting molecules

TSG101, *UBE2N*, *VPS28*, *EGFR* and *MDM2* that possibly interact with LRSAM1 were identified using the protein-protein interaction database STRING (Fig 3) and IntAct. After literature based evaluation these molecules were selected for further analysis. Furthermore, the AP-3 was selected for analysis since in a recent study LRSAM1 immunoprecipitated with AP-3 [14].

RNA expression analysis of interacting molecules in lymphoblastoid cell lines

We investigated RNA expression of candidate interacting molecules (*TSG101*, *UBE2N*, *VPS28*, *EGFR*, *MDM2* and *AP-3*) in the CMT2P patient and three control individuals' lymphoblastoid cell lines. mRNA levels of *TSG101*, *UBE2N*, *VPS28*, *MDM2* and *EGFR* were significantly reduced in the patient lymphoblastoid cell line as compared to the control, while *AP-3* presented an equal expression in both patient and control lymphoblastoid cell lines. Specifically, the patient sample showed significantly lower mRNA levels of *TSG101* (43%), *UBE2N* (45%), *VPS28* (32%), *EGFR* (41%) and *MDM2* (35%) as compared to the control sample. In contrast *AP-3* (98%) showed a similar expression between the patient and control samples (Fig 4).

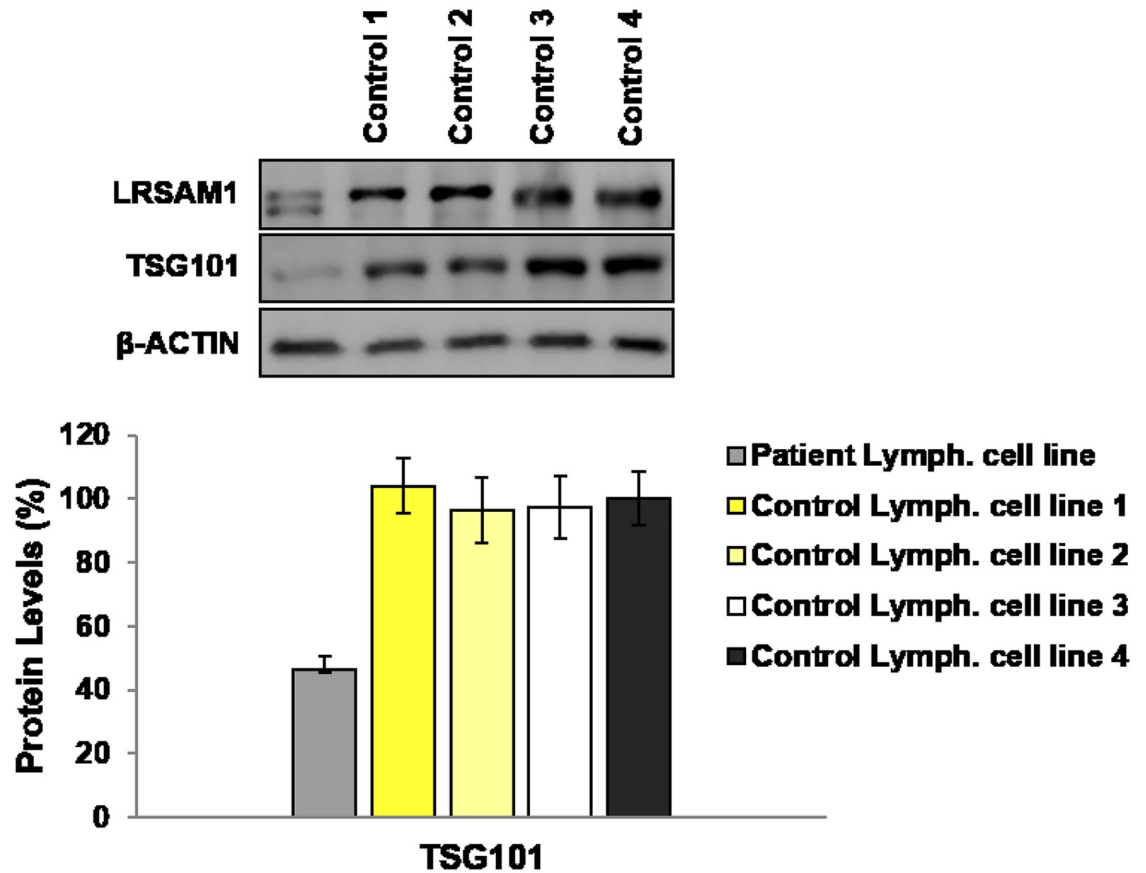


Fig 1. Investigation of TSG101 levels in lymphoblastoid cell lines. Western blot analysis of TSG101 protein levels in the patient and control individuals (1, 2, 3 and 4) lymphoblastoid cell lines. β -ACTIN was used as an internal control. Quantification of TSG101 was performed relative to β -ACTIN. The average of all control individuals values were set to 100%. **TSG101 levels:** Patient lymphoblastoid cell line ($47 \pm 4.09\%$, $p < 0.01456$), Control 1 lymphoblastoid cell line ($104 \pm 8.73\%$), Control 2 lymphoblastoid cell line ($96 \pm 10.34\%$), Control 3 lymphoblastoid cell line ($97 \pm 9.80\%$), Control 4 lymphoblastoid cell line ($100 \pm 8.38\%$).

<https://doi.org/10.1371/journal.pone.0211814.g001>

RNA expression analysis of interacting molecules in *LRSAM1* or *TSG101* downregulated SH-SY5Y cells

RNA expression of the above candidate molecules was evaluated in *LRSAM1* or *TSG101* downregulated cells as well. Ninety-six hours after the first *LRSAM1* siRNA transfection, we observed an approximately 70% reduction of endogenous *LRSAM1* RNA levels, reproducing the previously reported effect (5). Downregulation of *LRSAM1* also caused a significant decrease in approximately 50% of *TSG101*, *UBE2N*, *VPS28*, *MDM2* and *EGFR* mRNA expression. In agreement with findings in the patient derived lymphoblastoid cell line, *AP-3* mRNA levels were not affected by the *LRSAM1* downregulation. Ninety-six hours after the first *TSG101* siRNA transfection, we observed an approximately 70% reduction of endogenous *TSG101* RNA levels. Downregulation of *TSG101* caused an approximately 50% reduction of *VPS28* and a 20% decrease of *MDM2* levels. Normal levels of *LRSAM1*, *UBE2N*, *EGFR* and *AP-3* were observed after *TSG101* down regulation (Fig 5). Although, *LRSAM1* downregulation caused a significant reduction of TSG101 levels (55%), *TSG101* downregulation did not affect the expression of *LRSAM1*.

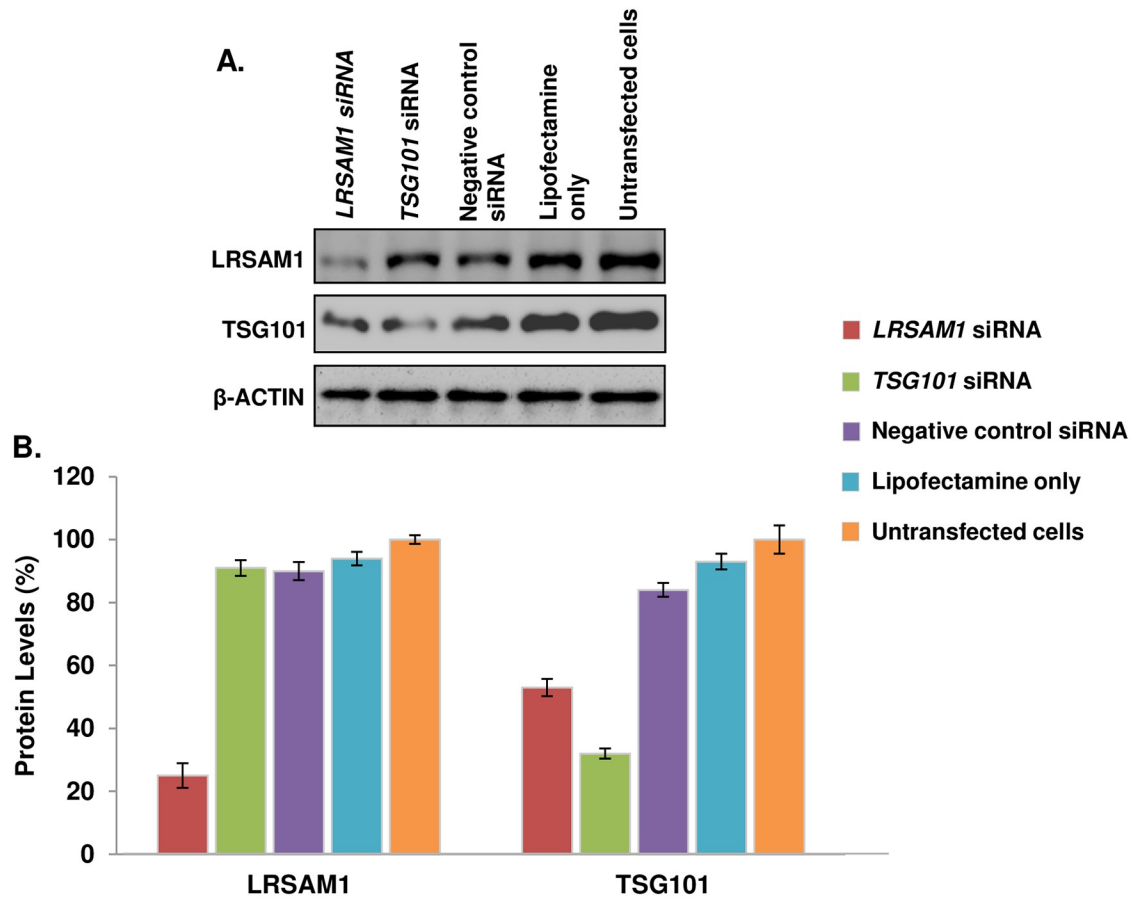


Fig 2. Efficiency of *LRSAM1* and *TSG101* downregulation. (A) Western blot analysis of LRSAM1 and TSG101 levels, compared with the controls (Negative control siRNA, Lipofectamine only, Untransfected cells) 96 hours after the first transfection. β -ACTIN was used as an internal control. (B) Quantification of LRSAM1 and TSG101 was performed relative to β -ACTIN. Untransfected cells values (LRSAM1 and TSG101) were set to 100% and reflect the normal protein levels within the 5 days of the experimental procedure. **LRSAM1 levels:** *LRSAM1* siRNA transfected cells ($25 \pm 3.94\%$, $p < 0.004$), *TSG101* siRNA transfected cells ($91 \pm 2.47\%$, $p < 0.0244$), Negative control siRNA transfected cells ($90 \pm 2.89\%$, $p < 0.009$), Lipofectamine only transfected cells ($94 \pm 2.15\%$, $p < 0.008$) and Untransfected cells ($100 \pm 1.36\%$). **TSG101 levels:** *LRSAM1* siRNA transfected cells ($53 \pm 2.72\%$, $p < 0.007$), *TSG101* siRNA transfected cells ($32 \pm 1.64\%$, $p < 0.0174$), Negative control siRNA transfected cells ($84 \pm 2.20\%$, $p < 0.027$), Lipofectamine only transfected cells ($93 \pm 2.49\%$, $p < 0.040$) and Untransfected cells ($100 \pm 4.51\%$).

<https://doi.org/10.1371/journal.pone.0211814.g002>

Discussion

LRSAM1 has been associated with CMT disease and currently its role in neurodegenerative disorders and in CMT pathogenesis is still unclear. In the present study we found that deregulation of *LRSAM1* impaired *TSG101*, *UBE2N*, *VPS28*, *MDM2* and *EGFR* levels. *TSG101* downregulation had an effect on *VPS28* and *MDM2* levels.

The E3 ligase activity of LRSAM1 performs ubiquitination of TSG101, regulating its expression [5]. TSG101 levels are also modulated by other mechanisms beyond LRSAM1 E3 regulation. MDM2, another E3 ligase, shares an autoregulatory loop with TSG101 [15]. TSG101 prevents its ubiquitination and increases the levels of MDM2 thus promoting ubiquitin degradation of p53 [15,16]. Over expression of truncated TSG101 in U20S cells caused reduction of MDM2 levels [15], while over expression of normal TSG101 doubled the short half-life of MDM2 and elevated its expression levels [15]. Notably we detected that 70% downregulation of *LRSAM1* caused 55% decrease in *TSG101* and also 55% decrease in *MDM2*, whereas 70%

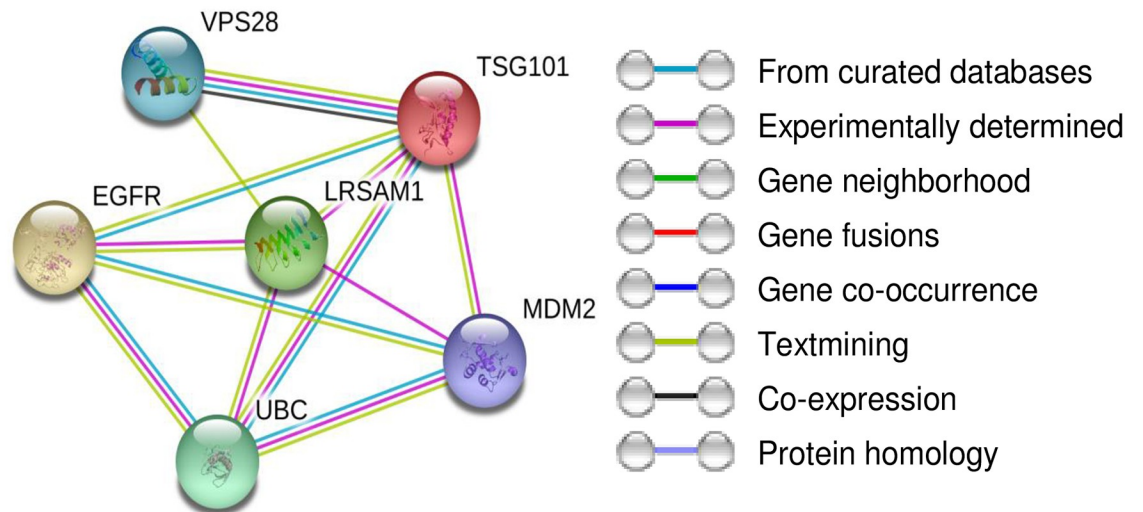


Fig 3. Protein-protein interaction network determined by STRING analysis for LRSAM1 protein. The interaction sources textmining, experiments, databases, co-expression, neighborhood, gene fusion and co-occurrence were used for the selection of the proteins.

<https://doi.org/10.1371/journal.pone.0211814.g003>

downregulation of *TSG101*, which did not affect *LRSAM1*, caused only 20% decrease in *MDM2* expression. These results indicate that *TSG101* exerts a small effect on *MDM2* expression (20%) relative to the effect of *LRSAM1* (55%), the later through an unknown mechanism.

Interaction of *TSG101* (yeast *VPS23*) with *VPS28*, *VPS37* and *MVB12* is necessary for the formation of the ESCRT-I complex [17]. Binding between *TSG101* and ESCRT-I subunits protects *TSG101* degradation [9]. *VPS28* binds to the C-Terminal of *TSG101* and blocks the

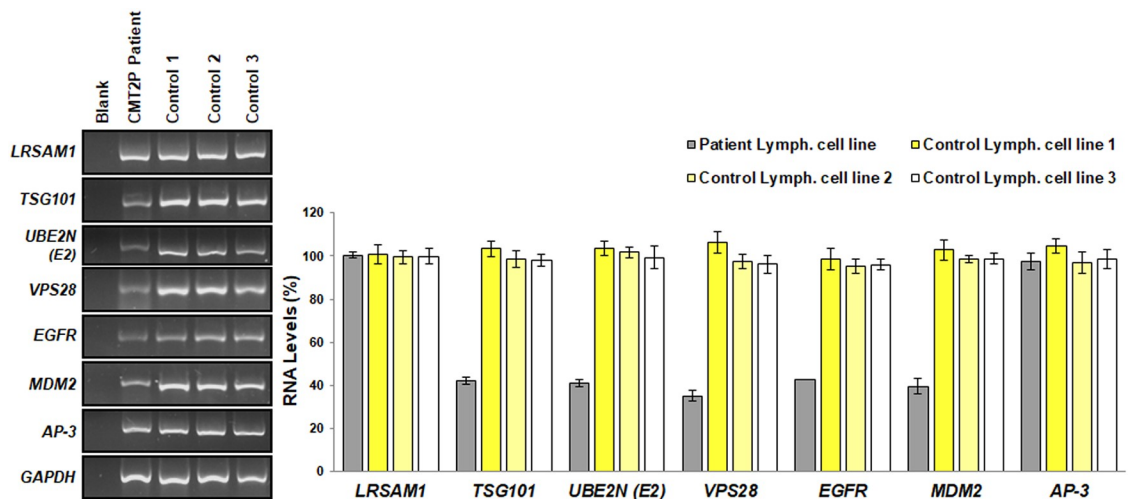


Fig 4. Investigation of LRSAM1 interacting molecules in the CMT2P patient lymphoblastoid cell line. (A) RNA expression analysis of most likely interacting molecules in patient and three control individuals' samples. *GAPDH* was used as a housekeeping internal control. (B) Quantification of the mRNA expression levels of the molecules relative to the control samples. The average of controls 1 to 3 was set to 100. Values were obtained as ratios of the RNA of interest over *GAPDH* control. Specifically, the patient lymphoblastoid cell line showed significantly lower levels of *TSG101* ($42.21\% \pm 1.62\%$, $p < 0.0007$), *UBE2N* ($40.94\% \pm 1.90\%$, $p < 0.005$), *VPS28* ($35.14\% \pm 2.62\%$, $p < 0.001$), *EGFR* ($42.58\% \pm 0.21\%$, $p < 0.003$) and *MDM2* ($39.44\% \pm 3.55\%$, $p < 0.0008$) than the control samples. In contrast *AP-3* ($97.34\% \pm 3.98\%$, $p < 0.104$) showed similar expression between the patient and control samples. Amplification of each primer set was repeated in triplicate.

<https://doi.org/10.1371/journal.pone.0211814.g004>

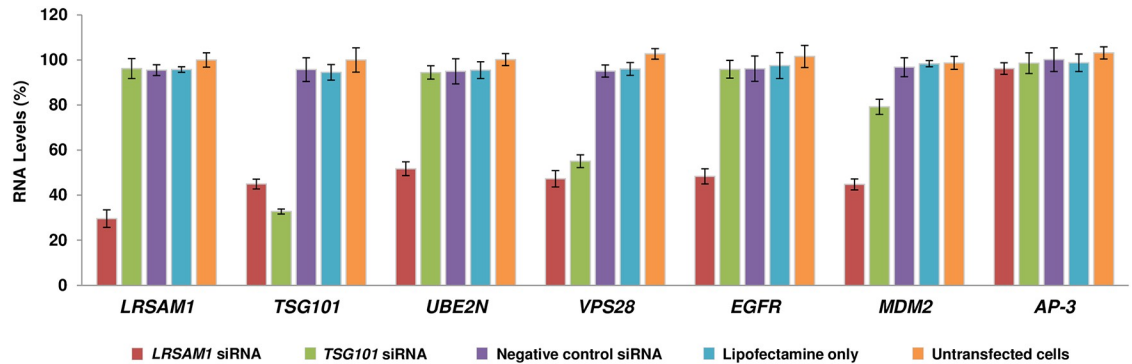


Fig 5. Investigation of LRSAM1 interacting molecules in LRSAM1 or TSG101 downregulated cells. Quantification of the RNA expression levels of the interacting molecules relative to the Untransfected control cells, which was set to 100 96h after the first siRNA transfection. Values were obtained as ratios of the RNA of interest over GAPDH control. Specifically, **LRSAM1 downregulation** significantly decreased the levels of *LRSAM1* ($30\% \pm 3.86\%$, $p < 0.0275$), *TSG101* ($45\% \pm 2.19\%$, $p < 0.0092$), *UBE2N* ($52\% \pm 3.05\%$, $p < 0.0158$), *VPS28* ($47\% \pm 3.62\%$, $p < 0.0336$), *EGFR* ($49\% \pm 3.38\%$, $p < 0.0125$) and *MDM2* ($45\% \pm 2.44\%$, $p < 0.0096$) compared to the Untransfected control cells. In contrast, *AP-3* ($96\% \pm 2.59\%$, $p < 0.0109$) showed similar expression between the *LRSAM1* knocked down and Untransfected cells. **TSG101 downregulation** significantly decreased the levels of *TSG101* ($33\% \pm 1.11\%$, $p < 0.0068$) and *VPS28* ($55\% \pm 2.86\%$, $p < 0.0154$) and also caused a small decrease of *MDM2* ($79\% \pm 3.37\%$, $p < 0.0217$) compared to the Untransfected cells. Expression levels of *LRSAM1* ($96\% \pm 4.41\%$, $p < 0.0427$), *UBE2N* ($94\% \pm 2.97\%$, $p < 0.0172$), *EGFR* ($96\% \pm 3.96\%$, $p < 0.0298$) and *AP-3* ($99\% \pm 4.57\%$, $p < 0.0462$) were similar to the Untransfected cells.

<https://doi.org/10.1371/journal.pone.0211814.g005>

interaction with LRSAM1, thus subsequently decreases the ubiquitination of TSG101 [18]. Reduced levels of VPS28 were observed in cells that lack TSG101 [18], while over expression of VPS28 did not affect the levels of TSG101 [9]. In our study, we observed decreased levels of VPS28 in the CMT2P patient lymphoblastoid cell line and showed that down regulation of LRSAM1 or TSG101 caused a significant reduction in VPS28 levels. It is thus possible that mutant or knockdown LRSAM1 affects VPS28 levels directly or through the impaired TSG101 levels. TSG101 and/or VSP28 deficiency possibly affect the formation of the ESCRT-I complex. The ESCRT-I complex along with ESCRT-0, ESCRT-II and ESCRT-III form the endosomal sorting complexes required for transport (ESCRTs). Each ESCRT complex, consists of VPS proteins, and regulates biogenesis of the Multivesicular Body (MVB) and cargo sorting within the lysosomes. Besides endocytic trafficking, tumor suppression, autophagy, miRNA function and cancer, the ESCRT has been associated with neurodegenerative diseases [19,20]. In the central nervous system endosomal trafficking and lysosomal functions are necessary processes for the survival of neurons. A recent study showed that, lack of Hrs (component of ESCRT-I) caused accumulation of ubiquitinated protein and neurodegeneration in the central nervous system of a mouse model [21]. In addition, mutated CHMP2B (component of ESCRT-III) leads to Frontotemporal dementia linked to chromosome 3 (FTD-3) because of autophagosome and ubiquitinated protein accumulation [20]. It is thus possible that dysregulation of any ESCRT complex can affect the normal function of the ESCRT machinery and the central nervous system.

We observed a decreased expression of *UBE2N* in the patient lymphoblastoid cell line and also in *LRSAM1* downregulated cells. A recent study showed, using a ubiquitination assay, that LRSAM1 interacts with UBC13, a mouse homolog of UBE2N and that mutations of LRSAM1 prevent this interaction, abolishing the ubiquitination activity of LRSAM1 [10]. UBE2N belongs to the family of Ubiquitin-conjugating enzymes (E2) and it is the only known enzyme that facilitates the creation of K63-linked polyubiquitination chains on proteins which are selected for proteasomal degradation [22,23]. E2 along with E1 and E3 enzymes consist the Ubiquitin-Proteasome System (UPS) system which removes the misfolded and abnormal proteins within the cells. Alzheimer, Parkinson and Huntington neurodegenerative diseases are

caused by the formation of inclusions in the brain because of the accumulation of misfolded proteins in neurons [23], indicating a possible pathogenic role of the UPS system in neurodegeneration. Expression of UBE2N was found to be elevated in synaptosomes in tissues obtained from aged monkey brain while UPS activity was found to be depressed. The increased level of UBE2N in aged monkey brain or the over expressed UBE2N in HEK293 cells, caused the accumulation of mutant huntingtin (HTT). In contrast, the decreased level of UBE2N in aged monkey brain, HEK293 and PC12 cells caused reduction of mutant HTT accumulation [23]. Knockdown of UBE2N in Parkin transfected HeLa cells inhibited the K63-linked polyubiquitination at mitochondrial sites suggesting a contribution of UBE2N in Parkin-mediated mitophagy [24]. The decreased expression of *UBE2N* observed in our study in LRSAM1 dysregulated cells indicates a possible synergistic role of UBE2N and LRSAM1 within the ubiquitin proteasome pathway.

The RING finger domain of LRSAM1 also plays a role in the regulation of EGFR expression [5]. We observed that the LRSAM1 c.2047-1G>A mutation, located in the RING finger domain, results in impaired *EGFR* expression in the CMT2P patient derived lymphoblastoid cells. In addition, *EGFR* expression was impaired by *LRSAM1* downregulation in the SH-SY5Y cells. Transfection of an inactive mutant-RING LRSAM1 has been reported to lead to the reduction of EGFR expression, while transfection of wild type LRSAM1 improved EGFR expression [5]. Also in the presence of mutant TSG101 in NIH 3T3 and SL6 cells, EGFR moved from the early endosomes and MVBs to the plasma membrane for recycling [25]. In our study, downregulation of *TSG101* did not affect the expression of *EGFR*. The EGF receptor is a family member of the ErbB receptors of kinases and regulates essential signaling pathways including cell proliferation and differentiation, cell cycle and migration [26]. Upregulation of EGFR has been associated with both oncogenesis and neurodegeneration. Expression of EGFR is activated in many malignancies such as breast cancer, prostate cancer and gliomas [27] and stimulates growth and differentiation of neurons [28]. Increased levels of the EGFR ligand promoted neuronal death, while high EGFR immunoreactivity was detected in neurites near the neuritic plaques of Alzheimer disease. Lack of Presenilin (PS1), a regulator of EGFR expression, increased EGFR levels resulting to abnormal cell cycle re-entrance [27,28]. Our data supports a role of dysregulated LRSAM1 in the deregulation of *EGFR*.

AP-3 has been reported to form a heterotetrameric complex, targeting cargos of lysosomes and lysosome related organelles [29]. Recently LRSAM1 was identified as an AP-3 interactor, because it immunoprecipitated with AP-3. It has been proposed, that while LRSAM1 is bound to AP-3, it regulates the ESCRT-I sorting function, by ubiquitinating certain cargoes [14]. We found normal mRNA expression of AP-3 in the CMT2P patient lymphoblastoid cell line as well as after *LRSAM1* downregulation in SH-SY5Y cells. These data, suggest that the interaction between the two molecules is probably controlled by AP-3 and not LRSAM1.

In conclusion, we confirm that *TSG101* expression is regulated by LRSAM1. Decreased levels of *UBE2N* and *EGFR* were observed only after *LRSAM1* knockdown thus indicating that these two molecules are regulated by a mechanism in which only LRSAM1 is involved. Decreased expression of *VPS28* and *MDM2* after either *LRSAM1* or *TSG101* downregulation demonstrates that the levels of these two molecules are regulated by a mechanism in which both LRSAM1 and TSG101 may be involved. Further investigation of the above molecules may enable delineation of the pathways that lead to CMT2P pathology.

Supporting information

S1 Fig. Quantitative analysis of possibly LRSAM1 interacting molecules. Standard curves were used to determine the cycles of the exponential phase for each set of primers used in the

RNA expression analysis. (A) *LRSAM1*-a: 37 cycles, (B) *LRSAM1*-b: 38 cycles, (C) *TSG101*-a: 33 cycles, (D) *TSG101*-b: 33 cycles, (E) *UBE2N*-a: 31 cycles, (F) *UBE2N*-a: 34 cycles, (G) *VPS28*-a: 32 cycles, (H) *VPS28*-b: 35 cycles, (I) *EGFR*-a: 37 cycles, (J) *EGFR*-b: 33 cycles, (K) *MDM2*-a: 33 cycles, (L) *MDM2*-b: 33 cycles, (M) *AP3*-a: 31 cycles, (N) *AP3*-b: 36 cycles (O) *GAPDH*: 24 cycles.
(PDF)

Author Contributions

Conceptualization: Anna Minaidou, Paschalis Nicolaou, Kyproula Christodoulou.

Data curation: Anna Minaidou, Paschalis Nicolaou, Kyproula Christodoulou.

Formal analysis: Anna Minaidou, Paschalis Nicolaou.

Funding acquisition: Anna Minaidou, Paschalis Nicolaou, Kyproula Christodoulou.

Investigation: Anna Minaidou, Paschalis Nicolaou, Kyproula Christodoulou.

Methodology: Anna Minaidou, Paschalis Nicolaou, Kyproula Christodoulou.

Project administration: Kyproula Christodoulou.

Resources: Kyproula Christodoulou.

Software: Anna Minaidou, Paschalis Nicolaou.

Supervision: Paschalis Nicolaou, Kyproula Christodoulou.

Validation: Anna Minaidou, Paschalis Nicolaou.

Visualization: Anna Minaidou, Paschalis Nicolaou.

Writing – original draft: Anna Minaidou.

Writing – review & editing: Anna Minaidou, Paschalis Nicolaou, Kyproula Christodoulou.

References

1. Shy ME, Patzko A (2011) Axonal Charcot-Marie-Tooth disease. *Curr Opin Neurol* 24: 475–483. <https://doi.org/10.1097/WCO.0b013e32834aa331> PMID: 21892080
2. Nicolaou P, Zamba-Papanicolaou E, Koutsou P, Kleopa KA, Georghiou A, et al. (2010) Charcot-Marie-Tooth disease in Cyprus: epidemiological, clinical and genetic characteristics. *Neuroepidemiology* 35: 171–177. <https://doi.org/10.1159/000314351> PMID: 20571287
3. Barisic N, Claeys KG, Sirotkovic-Skerlev M, Lofgren A, Nelis E, et al. (2008) Charcot-Marie-Tooth disease: a clinico-genetic confrontation. *Ann Hum Genet* 72: 416–441. <https://doi.org/10.1111/j.1469-1809.2007.00412.x> PMID: 18215208
4. Li B, Su Y, Ryder J, Yan L, Na S, et al. (2003) RIFLE: a novel ring zinc finger-leucine-rich repeat containing protein, regulates select cell adhesion molecules in PC12 cells. *J Cell Biochem* 90: 1224–1241. <https://doi.org/10.1002/jcb.10674> PMID: 14635195
5. Amit I, Yakir L, Katz M, Zwang Y, Marmor MD, et al. (2004) Tal, a Tsg101-specific E3 ubiquitin ligase, regulates receptor endocytosis and retrovirus budding. *Genes Dev* 18: 1737–1752. <https://doi.org/10.1101/gad.294904> PMID: 15256501
6. Engholm M, Sekler J, Schondorf DC, Arora V, Schittenhelm J, et al. (2014) A novel mutation in *LRSAM1* causes axonal Charcot-Marie-Tooth disease with dominant inheritance. *BMC Neurol* 14: 118. <https://doi.org/10.1186/1471-2377-14-118> PMID: 24894446
7. Guernsey DL, Jiang H, Bedard K, Evans SC, Ferguson M, et al. (2010) Mutation in the gene encoding ubiquitin ligase *LRSAM1* in patients with Charcot-Marie-Tooth disease. *PLoS Genet* 6.
8. Oh H, Mammucari C, Nenci A, Cabodi S, Cohen SN, et al. (2002) Negative regulation of cell growth and differentiation by TSG101 through association with p21(Cip1/WAF1). *Proc Natl Acad Sci U S A* 99: 5430–5435. <https://doi.org/10.1073/pnas.082123999> PMID: 11943869

9. McDonald B, Martin-Serrano J (2008) Regulation of Tsg101 expression by the steadiness box: a role of Tsg101-associated ligase. *Mol Biol Cell* 19: 754–763. <https://doi.org/10.1091/mbc.E07-09-0957> PMID: 18077552
10. Hakonen JE, Sorrentino V, Avagliano Trezza R, Wissel MB, van den Berg M, et al. (2017) LRSAM1-mediated ubiquitylation is disrupted in axonal Charcot-Marie-Tooth disease 2P. *Hum Mol Genet* 26: 2034–2041. <https://doi.org/10.1093/hmg/ddx089> PMID: 28335037
11. Nicolaou P, Cianchetti C, Minaidou A, Marrosu G, Zamba-Papanicolaou E, et al. (2013) A novel LRSAM1 mutation is associated with autosomal dominant axonal Charcot-Marie-Tooth disease. *Eur J Hum Genet* 21: 190–194. <https://doi.org/10.1038/ejhg.2012.146> PMID: 22781092
12. Minaidou A, Nicolaou P, Christodoulou K (2018) LRSAM1 Depletion Affects Neuroblastoma SH-SY5Y Cell Growth and Morphology: The LRSAM1 c.2047-1G>A Loss-of-Function Variant Fails to Rescue The Phenotype. *Cell J* 20.
13. Zhao G, Song J, Yang M, Song X, Liu X (2018) A novel mutation of LRSAM1 in a Chinese family with Charcot-Marie-Tooth disease. *J Peripher Nerv Syst* 23: 55–59. <https://doi.org/10.1111/jns.12247> PMID: 29341362
14. Traikov S, Stange C, Wassmer T, Paul-Gilloteaux P, Salamero J, et al. (2014) Septin6 and Septin7 GTP binding proteins regulate AP-3- and ESCRT-dependent multivesicular body biogenesis. *PLoS One* 9: e109372. <https://doi.org/10.1371/journal.pone.0109372> PMID: 25380047
15. Li L, Liao J, Ruland J, Mak TW, Cohen SN (2001) A TSG101/MDM2 regulatory loop modulates MDM2 degradation and MDM2/p53 feedback control. *Proc Natl Acad Sci U S A* 98: 1619–1624. <https://doi.org/10.1073/pnas.98.4.1619> PMID: 11172000
16. Ganguli G, Wasylyk B (2003) p53-independent functions of MDM2. *Mol Cancer Res* 1: 1027–1035. PMID: 14707286
17. Kostelansky MS, Schluter C, Tam YY, Lee S, Ghirlando R, et al. (2007) Molecular architecture and functional model of the complete yeast ESCRT-I heterotetramer. *Cell* 129: 485–498. <https://doi.org/10.1016/j.cell.2007.03.016> PMID: 17442384
18. Doyotte A, Russell MR, Hopkins CR, Woodman PG (2005) Depletion of TSG101 forms a mammalian "Class E" compartment: a multicisternal early endosome with multiple sorting defects. *J Cell Sci* 118: 3003–3017. <https://doi.org/10.1242/jcs.02421> PMID: 16014378
19. Saksena S, Wahlman J, Teis D, Johnson AE, Emr SD (2009) Functional reconstitution of ESCRT-III assembly and disassembly. *Cell* 136: 97–109. <https://doi.org/10.1016/j.cell.2008.11.013> PMID: 19135892
20. Lee JA, Gao FB (2012) Neuronal Functions of ESCRTs. *Exp Neurobiol* 21: 9–15. <https://doi.org/10.5607/en.2012.21.1.9> PMID: 22438674
21. Tamai K, Toyoshima M, Tanaka N, Yamamoto N, Owada Y, et al. (2008) Loss of hrs in the central nervous system causes accumulation of ubiquitinated proteins and neurodegeneration. *Am J Pathol* 173: 1806–1817. <https://doi.org/10.2353/ajpath.2008.080684> PMID: 19008375
22. Cheng J, Fan YH, Xu X, Zhang H, Dou J, et al. (2014) A small-molecule inhibitor of UBE2N induces neuroblastoma cell death via activation of p53 and JNK pathways. *Cell Death Dis* 5: e1079. <https://doi.org/10.1038/cddis.2014.54> PMID: 24556694
23. Yin P, Tu Z, Yin A, Zhao T, Yan S, et al. (2015) Aged monkey brains reveal the role of ubiquitin-conjugating enzyme UBE2N in the synaptosomal accumulation of mutant huntingtin. *Hum Mol Genet* 24: 1350–1362. <https://doi.org/10.1093/hmg/ddu544> PMID: 25343992
24. Geisler S, Vollmer S, Golombek S, Kahle PJ (2014) The ubiquitin-conjugating enzymes UBE2N, UBE2L3 and UBE2D2/3 are essential for Parkin-dependent mitophagy. *J Cell Sci* 127: 3280–3293. <https://doi.org/10.1242/jcs.146035> PMID: 24906799
25. Babst M, Odorizzi G, Estepa EJ, Emr SD (2000) Mammalian tumor susceptibility gene 101 (TSG101) and the yeast homologue, Vps23p, both function in late endosomal trafficking. *Traffic* 1: 248–258. PMID: 11208108
26. Webster RJ, Giles KM, Price KJ, Zhang PM, Mattick JS, et al. (2009) Regulation of epidermal growth factor receptor signaling in human cancer cells by microRNA-7. *J Biol Chem* 284: 5731–5741. <https://doi.org/10.1074/jbc.M804280200> PMID: 19073608
27. Teixeira AL, Gomes M, Medeiros R (2012) EGFR signaling pathway and related-miRNAs in age-related diseases: the example of miR-221 and miR-222. *Front Genet* 3: 286. <https://doi.org/10.3389/fgene.2012.00286> PMID: 23233863
28. Currais A, Hortobagyi T, Soriano S (2009) The neuronal cell cycle as a mechanism of pathogenesis in Alzheimer's disease. *Aging (Albany NY)* 1: 363–371.
29. Le Borgne R, Alconada A, Bauer U, Hoflack B (1998) The mammalian AP-3 adaptor-like complex mediates the intracellular transport of lysosomal membrane glycoproteins. *J Biol Chem* 273: 29451–29461. PMID: 9792650